Orthonormal Vector Fitting: A Robust Macromodeling Tool for Rational Approximation of Frequency Domain Responses

Dirk Deschrijver, Bart Haegeman, and Tom Dhaene

Abstract—Vector Fitting is widely accepted as a robust macromodeling tool for approximating frequency domain responses of complex physical structures. In this paper, the Orthonormal Vector Fitting technique is presented, which uses orthonormal rational functions to improve the numerical stability of the method. This reduces the numerical sensitivity of the system equations to the choice of starting poles significantly and limits the overall macromodeling time.

Index Terms—Macromodeling, rational functions, system identification.

I. INTRODUCTION

ACCURATE frequency-domain macromodels are becoming increasingly important for the design, study, and optimization of complex physical structures, such as, e.g., electronic packages. These compact macromodels approximate the complex electromagnetic (EM) behavior of high-speed multiport systems at the input and output ports in the frequency domain by rational functions. Rational linear least-squares approximation techniques are often applied to identify the model parameters; however, they are known to suffer from poor numerical conditioning if the frequency range is rather broad, or when the macromodel requires a large amount of poles.

Gustavsen and Semlyen recently proposed an iterative macromodeling technique, called vector fitting (VF) [1], which is basically a reformulation of the Sanathanan–Koerner (SK) iteration [2] using a partial fraction basis [3]. Initially, the poles of these partial fractions are prescribed, and they are relocated in successive iterations until the SK iteration is converged. The robustness of the method is mainly due to the use of rational bases instead of polynomials, which are numerically advantageous if the prescribed poles are properly chosen. This method has been widely applied in many scientific communities, such as power systems and microwave engineering.

In this paper, the Orthonormal Vector Fitting (OVF) technique [4] is presented, which is numerically more robust than the classical VF algorithm. It is shown that the use of orthonormal rational functions makes the system equations significantly better conditioned, especially when the initial poles are not chosen in an optimal way. Since the poles are identified more accurately,

less iterations are needed, and the overall macromodeling time can be reduced. The computational complexity of both methods is approximately the same per iteration. Once the rational model is identified, it is represented as a state-space realization, and can easily be converted to a SPICE or EMTP circuit.

First, the new iterative method is placed in a broader context of macromodeling and it is related to some of the existing work. Afterwards, the technique is described in detail and the robustness is illustrated by a simulation-based example. The Appendices offer a more thorough analysis for the interested reader.

II. IDENTIFICATION ALGORITHM

A. Goal

The major goal of macromodeling is to identify the mapping between the inputs and outputs of a complex system by an analytic model. For continuous-time linear time invariant (LTI) systems in the frequency domain, this reduces to finding a rational transfer function

$$R(s) = \frac{N(s)}{D(s)} = \frac{\sum_{n=0}^{N} N_n \phi_n(s)}{\sum_{d=0}^{D} D_d \phi_d(s)} \quad s = i2\pi f \quad (1)$$

which approximates the spectral response of a system over some predefined frequency range of interest $[f_{\min}, f_{\max}]$. The spectral behavior is characterized by a set of frequency-domain data samples $(s_k, H(s_k)), \forall k = 0, \ldots, K$, which can be obtained from observations, such as, e.g., measurements or circuit simulations [5].

N_n and D_d are the real-valued system parameters which need to be estimated, and N and D represent the order of numerator and denominator, respectively. In many situations, the amount of available data samples is quite numerous, so numerically stable fitting techniques are required which estimate the model coefficients in a least-squares sense [6].

B. Nonlinearity of the Estimator

Rational least-squares approximation is essentially a nonlinear problem, and corresponds to minimizing the following cost function [7]

$$\arg \min_{N_n, D_d} \sum_{k=0}^{K} \left| H(s_k) - \frac{N(s_k)}{D(s_k)} \right|^2$$

$$= \arg \min_{N_n, D_d} \sum_{k=0}^{K} \frac{1}{|D(s_k)|^2} |D(s_k)H(s_k) - N(s_k)|^2. \quad (2)$$

Due to its nonlinear nature, it becomes quite hard to estimate the system parameters in a fast and accurate way.

In many papers, e.g., [8], this difficulty is avoided by assuming that *a priori* knowledge about the poles is available. In this case, the nonlinear problem reduces to a linear problem since the denominator parameters are assumed to be known. In practice, however, this situation is often not a realistic one.

Another possible option is the use of nonlinear optimization techniques, such as Newton–Gauss type algorithms, in order to minimize (2). This approach is computationally not always efficient, and the solutions may converge to local minima, even when Levenberg–Marquardt algorithms are used to extend the region of convergence [9], [10].

In [11], it was proposed to minimize a Kalman-linearized cost function that is nonquadratic in the system parameters [12], [13]

$$\arg \min_{N_n, D_d} \sum_{k=0}^{K} |D(s_k)H(s_k) - N(s_k)|^2. \quad (3)$$

This formulation basically reduces to (2), if the weighting factor $\left(1/|D(s_k)|^2\right)$ is set equal to one for all frequencies s_k. Clearly, this weighting will bias the fitted transfer function, and this often results in poor low-frequency fits, due to an undesired overemphasis of high-frequency errors.

In this paper, the use of a Sanathanan–Koerner iteration is advocated [2]. First, an estimate of the poles is obtained by minimizing the Kalman-linearized cost function. Given this initial (iteration step 0) or previous (iteration step $t-1$) estimate of the poles, the model parameters of the next iteration step are calculated by minimizing the weighted linear cost function:

$$\arg \min_{N_n^{(t)}, D_d^{(t)}} \left(\sum_{k=0}^{K} \frac{1}{\left|D^{(t-1)}(s_k)\right|^2} \right.$$
$$\left. \times \left|D^{(t)}(s_k)H(s_k) - N^{(t)}(s_k)\right|^2 \right). \quad (4)$$

By analyzing the gradients of the error criterion, it is straightforward to show that this method generates solutions that do not converge asymptotically to the solution of (2) either, even though the error criterion itself tends asymptotically to the fundamental least squares criterion [14]. In practice, however, this approach often gives favorable results for sufficiently high signal-to-noise ratios and sufficiently small modeling errors.

The interested reader is hereby referred to an excellent survey [7] which analyzes these and several other techniques in more detail.

C. Choice of Basis Functions

To solve the identification problem, (4) reduces naturally to a linear set of least-squares equations, which needs to be solved with sufficient accuracy.

Suppose that $H = \operatorname{diag}(H(s_0), \ldots, H(s_K))$, $w_k = \left[D^{(t-1)}(s_k)\right]^{-1}$, and $\Phi_{0:X}$ is defined as

$$\Phi_{0:X} = \begin{pmatrix} w_0\phi_0(s_0) & \cdots & w_0\phi_X(s_0) \\ \cdots & \cdots & \cdots \\ w_K\phi_0(s_K) & \cdots & w_K\phi_X(s_K) \end{pmatrix}. \quad (5)$$

Then the least-squares solution of $Ax = b$ can be calculated to estimate the parameter vector x, provided that A, x and b are defined as ($D_0 = 1$)

$$A = \begin{pmatrix} \Re e\left(\Phi_{0:N} \quad -H\Phi_{1:D}\right) \\ \Im m\left(\Phi_{0:N} \quad -H\Phi_{1:D}\right) \end{pmatrix} \quad (6)$$

$$x = \left(N_0^{(t)} \ldots N_N^{(t)} D_1^{(t)} \ldots D_D^{(t)}\right)^T \quad (7)$$

$$b = \begin{pmatrix} \Re e(H\Phi_0) \\ \Im m(H\Phi_0) \end{pmatrix}. \quad (8)$$

Each equation is split in its real and imaginary part to enforce the poles and zeros to be real, or to occur in complex conjugate pairs (under the assumption that the basis functions $\phi(s)$ are real-valued as well). This ensures that the coefficients of the transfer function are real, and that no imaginary terms occur in the time-domain.

Now it's easy to estimate the system parameters by solving the normal equations

$$x = (A^T A)^{-1} A^T b \quad (9)$$

or, e.g., by using a QR decomposition with column pivoting, or a least-squares singular value decomposition (SVD), which are often more accurate.

It becomes clear that the accuracy of the parameter vector x and the numerical conditioning of this problem is highly dependent on the structure of the normal equations $A^T A$ [6]. If the basis functions $\phi(s)$ are chosen to be a monomial power series basis $(1, s, s^2, \ldots)$, the matrix Φ will be a Vandermonde matrix which is notoriously ill-conditioned.

Adcock and Potter [15] suggested the use of polynomials which are orthogonal with respect to a continuous inner product, such as Chebyshev polynomials, as basis functions. The large variation of the Chebyshev polynomials with increase in order makes it possible to downsize the effects of ill-conditioning.

On the other hand, Richardson and Formenti [16] proposed the use of Forsythe polynomials which are orthonormal with respect to a discrete inner product, defined by the normal equations of the estimator. This implies that a different set of basis functions is used for numerator and denominator. Rolain *et al.* [17] have shown that a basis transformation from the Forsythe polynomials to a different, arbitrary polynomial basis results in an inferior conditioning of $A^T A$. Hence, the Forsythe polynomial basis is optimal in a sense that there does not exist any other polynomial basis resulting in a better conditioned form of the normal equations.

III. VECTOR FITTING

Although polynomial bases are probably the most natural choice, it is well-known that rational basis functions have a lot of numerical advantages. Quite recently, Gustavsen and Semlyen [1] proposed the use of partial fractions as basis functions for the numerator and denominator

$$R(s) = \frac{\sum_{p=1}^{P} c_p \phi_p(s)}{1 + \sum_{p=1}^{P} \tilde{c}_p \phi_p(s)} = \frac{\sum_{p=1}^{P} \frac{c_p}{s + a_p}}{1 + \sum_{p=1}^{P} \frac{\tilde{c}_p}{s + a_p}} \quad (10)$$

provided that c_p and $\tilde{c}_p$ represent the residues, and $-a_p$ are a set of prescribed poles. The denominator has an additional basis function which equals the constant value 1. Its coefficient can be fixed to one, since numerator and denominator can be divided by the same constant value without loss of generality. Other nontriviality constraints are also possible [18]. Given the constraint that the poles of the numerator and denominator expression of (10) are the same, it is easy to see that these basis functions are complete, in a sense that they can approximate any strictly proper transfer function with distinct poles arbitrarily well. To approximate systems which require a proper or improper transfer function, an optional constant and linear term can be added to the numerator expression.

In the first iteration ($t = 0$), this choice of basis functions implies that A becomes

$$A = \begin{pmatrix} \Re e\,(\,\Phi_{1:P}) & -H\Phi_{1:P} \\ \Im m\,(\,\Phi_{1:P}) & -H\Phi_{1:P} \end{pmatrix} \tag{11}$$

and that the parameter vector consist of unknown residues

$$x = (c_1 \ldots c_P\ \tilde{c}_1 \ldots \tilde{c}_P)^T. \tag{12}$$

The Φ matrix is then a Cauchy matrix, which makes the normal equations often well-conditioned if the prescribed poles are well chosen. As suggested in [1] and [19], the poles are optimally selected as complex conjugate pairs on a vertical or skew line, close to the imaginary axis. Due to the iterative behavior of the SK-iteration, the prescribed poles are relocated until the poles converge in such way that the SK cost function is minimized. In general, this happens quite fast (i.e., < 3 iterations).

When poles are chosen too far to the left in the complex plane, the real part of the poles dominates the matrix entries, which deteriorates the numerical conditioning

$$\frac{1}{s_k + a_p} = \frac{1}{i\omega_k - i(\Im m(-a_p)) - \Re e(-a_p)} \tag{13}$$

$$\approx \frac{-1}{\Re e(-a_p)}. \tag{14}$$

Note, however, that for most physical systems, the real part of the poles is usually rather small. This means that the conditioning of the normal equations often improves as the SK-iteration relocates the poles to their optimal location. This process is described in more detail in Appendix A. Even when the initial poles are inappropriately chosen, the algorithm succeeds in minimizing (4), at the expense of additional iterations.

To make sure that the transfer function has real-valued coefficients, a linear combination of $\phi_p(s)$ and $\phi_{p+1}(s)$ is formed to make the residues $c_{p+1} = c_p^*$ complex conjugate if the poles $-a_{p+1} = -a_p^*$. This way, two basis functions of the following form are obtained:

$$\phi_p(s) = \frac{1}{(s + a_p)} + \frac{1}{(s + a_{p+1})} \tag{15}$$

$$\phi_{p+1}(s) = \frac{i}{(s + a_p)} - \frac{i}{(s + a_{p+1})}. \tag{16}$$

This causes the corresponding elements in the solution vector to become equal to $\Re e(c_p)$ and $\Im m(c_p)$. After parameterization of x, (10) can be simplified by cancelling out common poles. This means that the zeros of the denominator expression become the

poles of the final transfer function. Calculating the zeros can easily be done as follows.

The minimal LTI state-space realization

$$sX(s) = \mathrm{A}X(s) + \mathrm{B}U(s) \tag{17}$$

$$Y(s) = \mathrm{C}X(s) + \mathrm{D}U(s) \tag{18}$$

of the denominator

$$D(s) = \sum_{p=1}^{P} \frac{\tilde{c}_p}{s + a_p} + 1 \tag{19}$$

can be obtained by a parallel connection (initially $\mathrm{A}, \mathrm{B}, \mathrm{C} = \phi$ and $\mathrm{D} = 0$)

$$\mathrm{A} = \begin{pmatrix} \mathrm{A} & 0 \\ 0 & \mathrm{A}_p \end{pmatrix} \qquad \mathrm{B} = \begin{pmatrix} \mathrm{B} \\ \mathrm{B}_p \end{pmatrix}$$

$$\mathrm{C} = (\,\mathrm{C} \quad \mathrm{C}_p) \qquad \mathrm{D} = \mathrm{D} + \mathrm{D}_p \tag{20}$$

of the minimal state space realizations $(\mathrm{A}_p, \mathrm{B}_p, \mathrm{C}_p, \mathrm{D}_p)$ of each simple fraction, with

$$\mathrm{A}_p = -a_p, \qquad \mathrm{B}_p = 1, \quad \mathrm{C}_p = \tilde{c}_p, \quad \mathrm{D}_p = 0 \tag{21}$$

provided that $-a_p$ is real. If $-a_p$ and $-a_{p+1}$ constitute a complex conjugate pair of poles (i.e., $-a_{p+1} = -a_p^*$), the corresponding state space realization of the linear combination is given as

$$\mathrm{A}_p = \begin{pmatrix} \Re e(-a_p) & \Im m(-a_p) \\ -\Im m(-a_p) & \Re e(-a_p) \end{pmatrix} \qquad \mathrm{B}_p = \begin{pmatrix} 2 \\ 0 \end{pmatrix}$$

$$\mathrm{C}_p = (\,\Re e(\tilde{c}_p) \quad \Im m(\tilde{c}_p)\,) \qquad \mathrm{D}_p = 0. \tag{22}$$

Afterwards, the constant term 1 of (18) can simply be added to the scalar D. This transformation makes the state-space realization of $D(s)$

$$D(s) = \mathrm{C}(sI - \mathrm{A})^{-1}\mathrm{B} + \mathrm{D} \tag{23}$$

real-valued, such that the poles and zeros occur as complex conjugate pairs. The zeros of (23) can then be solved by calculating the eigenvalues of A-BC. After simplification of (10), these eigenvalues will become the relocated poles of the transfer function

$$-a_p = \mathrm{eig}(\mathrm{A} - \mathrm{BC}) \tag{24}$$

and this procedure can be iterated until the SK-cost function is minimized. Solving the residues becomes a linear problem, since the poles are now identified

$$\arg \min_{c_p} \sum_{k=0}^{K} \left| H(s_k) - \left(\sum_{p=1}^{P} \frac{c_p}{s_k + a_p} \right) \right|^2. \tag{25}$$

This technique was called "Vector Fitting" [1], and it has been widely applied to many modeling problems within power systems, high-speed interconnection structures, electronic packages, and microwave systems.

IV. ORTHONORMAL VECTOR FITTING

Instead of using the partial fractions as rational basis functions, it was shown that orthonormal rational basis functions can lead to significant improvements in numerical conditioning [20], [21]. A straightforward way to calculate an orthonormal basis, is to apply a Gram–Schmidt procedure on the partial fractions [11], [22], [23]. Hence, orthonormal rational functions $\phi_p(s)$ are obtained, which are in fact linear combinations of the partial fractions, of the form

$$\phi_p(s) = \frac{Q_p(s)}{\prod_{j=1}^{p}(s + a_j)} \quad (26)$$

for $p = 1, \ldots, P$ and $Q_p(s)$ an arbitrary polynomial of order $p - 1$, such that

$$\langle \phi_m(s), \phi_n(s) \rangle = \delta_{mn} \quad (27)$$

with $1 \leq m, n \leq P$. If the inner product is defined as

$$\langle \phi_m(s), \phi_n(s) \rangle = \frac{1}{2\pi i} \int_{i\mathbb{R}} \phi_m(s)\phi_n^*(s)ds \quad (28)$$

then the $Q_p(s)$ polynomial can be determined by imposing the orthonormality conditions on the basis functions. As an example, consider the construction of the first function: $\phi_1(s)$.

$$\langle \phi_1(s), \phi_1(s) \rangle = \frac{1}{2\pi i} \int_{i\mathbb{R}} \phi_1(s)\phi_1^*(s)ds \quad (29)$$

$$= \frac{1}{2\pi i} \int_{i\mathbb{R}} \frac{|\gamma_1|^2}{(s + a_1)(-s + a_1^*)}ds \quad (30)$$

$$= \frac{|\gamma_1|^2}{a_1 + a_1^*}. \quad (31)$$

To normalize $\phi_1(s)$, $Q_1(s) = \gamma_1$ must equal $\kappa_1 \sqrt{2\Re e(a_1)}$, where κ_1 is an arbitrary unimodular complex number. $\phi_1(s)$ is then obtained as

$$\phi_1(s) = \kappa_1 \sqrt{2\Re e(a_1)}\frac{1}{s + a_1}. \quad (32)$$

Now consider the construction of the second function $\phi_2(s)$. First of all, $\phi_2(s)$ must be orthogonal to $\phi_1(s)$

$$\langle \phi_1(s), \phi_2(s) \rangle = \frac{1}{2\pi i} \int_{i\mathbb{R}} \phi_1(s)\phi_2^*(s)ds = 0 \quad (33)$$

which implies that $\phi_2^*(s)$ must vanish for $s = -a_1$. Therefore, $Q_2(s) = \gamma_2(s - a_1^*)$. This constant γ_2 is determined by imposing the normalization condition

$$\langle \phi_2(s), \phi_2(s) \rangle = \frac{1}{2\pi i} \int_{i\mathbb{R}} \frac{\gamma_2(s - a_1^*)}{(s + a_1)(s + a_2)}$$
$$\times \frac{\gamma_2^*(-s - a_1)}{(-s + a_1^*)(-s + a_2^*)}ds \quad (34)$$

$$= \frac{1}{2\pi i} \int_{i\mathbb{R}} \frac{|\gamma_2|^2}{(s + a_2)(-s + a_2^*)}ds$$

$$= \frac{|\gamma_2|^2}{a_2 + a_2^*}. \quad (35)$$

Clearly, it follows that $\gamma_2 = \kappa_2 \sqrt{2\Re e(a_2)}$, where κ_2 is an arbitrary unimodular complex number. So, $\phi_2(s)$ is then given by

$$\phi_2(s) = \kappa_2 \sqrt{2\Re e(a_2)}\frac{s - a_1^*}{(s + a_1)(s + a_2)}. \quad (36)$$

Similarly continuing this approach, the general polynomials are obtained:

$$\phi_p(s) = \kappa_p \sqrt{2\Re e(a_p)} \left(\prod_{j=1}^{p-1} \frac{s - a_j^*}{s + a_j} \right) \frac{1}{s + a_p}. \quad (37)$$

This basis originates from the discrete-time Takenaka–Malmquist basis [24], [25], and has later been transformed to the continuous time domain. It is a generalization of the Laguerre basis [26], where all poles $\{-a_p\}$ are the same real number, and the two-parameter Kautz bases [27] where all poles $\{-a_p, -a_{p+1}\}$ are the same complex conjugate pair with $-a_p^* = -a_{p+1}$. A theoretical analysis of these basis functions is well described in literature. The interested reader is referred to [28] which gives an excellent survey.

To make sure that the transfer function has real-valued coefficients, a linear combination of $\phi_p(s)$ and $\phi_{p+1}(s)$ is formed which can be made real-valued if the poles are real or occur in a complex conjugate pair. This way, two orthonormal functions of the following form are obtained:

$$\phi_p(s) = \gamma_p \left(\prod_{j=1}^{p-1} \frac{s - a_j^*}{s + a_j} \right) \frac{s - x}{(s + a_p)(s + a_{p+1})} \quad (38)$$

$$\phi_{p+1}(s) = \gamma_{p+1} \left(\prod_{j=1}^{p-1} \frac{s - a_j^*}{s + a_j} \right) \frac{s - y}{(s + a_p)(s + a_{p+1})} \quad (39)$$

with real $\gamma_p, \gamma_{p+1}, x,$ and y. To impose the orthogonality

$$\langle \phi_p(s), \phi_{p+1}(s) \rangle = \gamma_p\gamma_{p+1} \frac{xy + a_p a_{p+1}}{2(a_p + a_{p+1})a_p a_{p+1}} = 0 \quad (40)$$

x and y are set to be $\sqrt{a_p a_{p+1}} = |a_p|$, and $-\sqrt{a_p a_{p+1}} = -|a_p|$, respectively. Similarly, γ_p and γ_{p+1} are set to $\sqrt{a_p + a_{p+1}} = \sqrt{2\Re e(a_p)}$. Note that this choice is not unique, and that other possibilities exist. Note also that the orthonormalization of the basis functions is done analytically instead of numerically, so it does not require any additional computation time.

The minimal continuous-time LTI state-space realization

$$sX(s) = AX(s) + BU(s) \quad (41)$$
$$Y(s) = CX(s) + DU(s) \quad (42)$$

of the denominator

$$D(s) = 1 + \sum_{p=1}^{P} \tilde{c}_p\phi_p(s) \quad (43)$$

can then be calculated by cascading the minimal state-space realization of smaller, first-, and second-order sections [29]

$$\frac{s-a_1^*}{s+a_1} \to \frac{s-a_2^*}{s+a_2} \to \cdots \to \frac{s-a_{P-1}^*}{s+a_{P-1}} \to \frac{1}{s+a_P}. \quad (44)$$

The minimal state-space realization (A_p, B_p, C_p, D_p) of the all-pass function

$$\frac{Y_p(s)}{U_p(s)} = \frac{s-a_p^*}{s+a_p} \quad (45)$$

for $p = 1, \ldots, P-1$ is given as

$$A_p = -a_p, \quad B_p = 1, \quad C_p = 2\Re e(-a_p), \quad D_p = 1 \quad (46)$$

and the minimal state-space realization (A_p, B_p, C_p, D_p) of the low-pass function

$$\frac{Y_p(s)}{U_p(s)} = \frac{1}{s+a_p} \quad (47)$$

is given as

$$A_p = -a_p, \quad B_p = 1, \quad C_p = 1, \quad D_p = 0 \quad (48)$$

for $p = P$. Then the minimal state-space realization of the compound system (44) is obtained as the cascade construction

$$A = \begin{bmatrix} A_1 & 0 & \ldots & 0 \\ B_2C_1 & A_2 & \ldots & 0 \\ B_3D_2C_1 & B_3C_2 & \ldots & 0 \\ B_4D_3D_2C_1 & B_4D_3C_2 & \ldots & 0 \\ \ldots & \ldots & \ldots & \ldots \\ B_PD_{P-1}\ldots D_2C_1 & B_PD_{P-1}\ldots D_3C_2 & \ldots & A_P \end{bmatrix}$$

$$B = \begin{bmatrix} B_1 \\ B_2D_1 \\ B_3D_2D_1 \\ B_4D_3D_2D_1 \\ \ldots \\ B_PD_{P-1}\ldots D_1 \end{bmatrix}$$

$$C = \begin{bmatrix} D_P \ldots D_2C_1 \\ D_P \ldots D_3C_2 \\ \ldots \\ C_P \end{bmatrix}^T$$

$$D = D_P \ldots D_1 \quad (49)$$

of the smaller state space models, with $y_p(t) = u_{p+1}(t)$.

The state matrix A and the input vector B are build such that the states contain exactly the unnormalized basis functions. The output vector C and scalar D are chosen to obtain the denominator expression (43), by compensating for the coefficients $\tilde{c}_p$

and normalization constant $\sqrt{2\Re e(a_p)}$ in the vector C, and setting the scalar D equal to the constant value 1. The following real-valued state space realization is obtained:

$$A_{P\times P} = \begin{bmatrix} -a_1 & 0 & 0 & \ldots & 0 \\ 2\Re e(-a_1) & -a_2 & 0 & \ldots & 0 \\ 2\Re e(-a_1) & 2\Re e(-a_2) & -a_3 & \ldots & 0 \\ 2\Re e(-a_1) & 2\Re e(-a_2) & 2\Re e(-a_3) & \ldots & 0 \\ \ldots & \ldots & \ldots & \ldots & \ldots \\ 2\Re e(-a_1) & 2\Re e(-a_2) & 2\Re e(-a_3) & \ldots & -a_P \end{bmatrix}$$

$$B_{1\times P} = \begin{bmatrix} 1 \\ 1 \\ \ldots \\ 1 \end{bmatrix}$$

$$C_{P\times 1} = \begin{bmatrix} \tilde{c}_1\sqrt{2\Re e(a_1)} \\ \tilde{c}_2\sqrt{2\Re e(a_2)} \\ \ldots \\ \tilde{c}_P\sqrt{2\Re e(a_P)} \end{bmatrix}^T$$

$$D_{1\times 1} = 1 \quad (50)$$

provided that the poles $-a_p$ are real.

If $-a_p$ and $-a_{p+1}$ constitute a complex conjugate pair of poles (i.e., $-a_{p+1} = -a_p^*$), a real-valued state-space realization is obtained by replacing

$$\frac{s-a_p^*}{s+a_p} \to \frac{s-a_{p+1}^*}{s+a_{p+1}} \quad (51)$$

in the cascade scheme (44) by

$$\frac{(s-a_p^*)(s-a_{p+1}^*)}{(s+a_p)(s+a_{p+1})} = 1 + \frac{4\Re e(-a_p)s}{(s+a_p)(s+a_p^*)}. \quad (52)$$

This corresponds to replacing

$$\begin{pmatrix} -a_p & 0 \\ 2\Re e(-a_p) & -a_{p+1} \end{pmatrix} \quad (53)$$

in the state matrix A by

$$\begin{pmatrix} \Re e(-a_p) & \Re e(-a_p) - |a_p| \\ \Re e(-a_p) + |a_p| & \Re e(-a_p) \end{pmatrix}. \quad (54)$$

The other state space matrices remain unchanged. Appendix B describes this transformation in more detail. Again, the zeros of the denominator are calculated by solving the eigenvalues of A-BC. These eigenvalues become a new set of prescribed poles, and the procedure is repeated iteratively until the SK cost function is converged. Afterwards, the identified poles can be used to determine the residues, which is essentially a linear problem. If the poles are stable, the residues can be estimated in the orthonormal basis

$$\arg\min_{c_p} \sum_{k=0}^{K} \left| H(s_k) - \left(\sum_{p=1}^{P} c_p\phi_p(s) \right) \right|^2. \quad (55)$$

If unstable poles are allowed, one can resort to the partial fraction basis

$$\arg\min_{c_p} \sum_{k=0}^{K} \left| H(s_k) - \left(\sum_{p=1}^{P} \frac{c_p}{s_k + a_p} \right) \right|^2. \quad (56)$$

Both representations can easily be realized to state-space as was shown before.
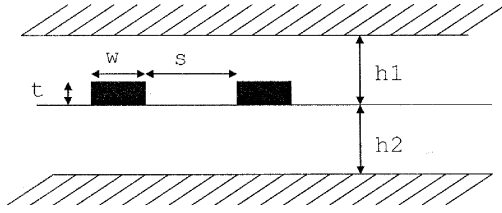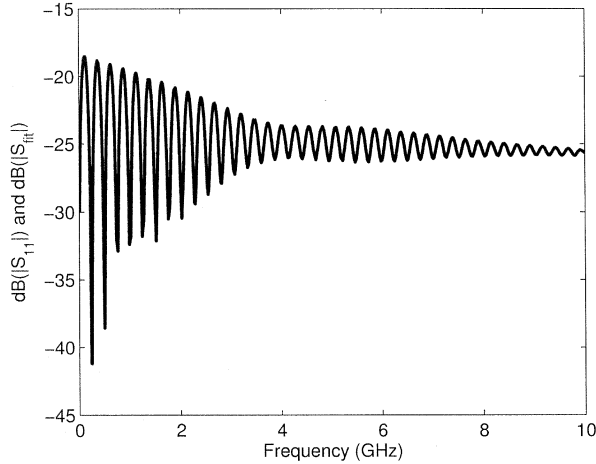
Fig. 1. Representation of striplines.

Fig. 2. Reflection coefficient (S_{11}) of lossy coupled lines.

Fig. 3. Error fitting model.

Nr. Iter.	Cond.Nr. VF	Cond.Nr. OVF
1	4.9687×10^{11}	4.9439×10^{11}
2	8.5875×10^{10}	2.0254×10^{8}
3	6.3612×10^{5}	5.8277×10^{4}
4	5.6283×10^{5}	5.4259×10^{4}

V. EXAMPLE

The reflection coefficient S_{11} of two symmetric coupled dispersive striplines (length = 13 000 mil, width = 7.501 mil, spacing = 9.502 mil, thickness = 0.36 mil, conductivity = $5.8 \cdot 10^7$ S/m)), laying inbetween two lossy substrate layers (substrate1: height = 13.9 mil, ε_r = 4.2, tg δ = 0.024 and substrate2: height = 5.24 mil, ε_r = 2.6, tg δ = 0.004), is modeled using the proposed technique. Fig. 1 shows the structure, and Fig. 2 shows the magnitude of the spectral response over the frequency range of interest [50 Hz–10 GHz].

First, a prescribed set of complex conjugate starting poles is chosen as was proposed by [1]

$$-a_p = -\alpha + \beta i, -a_{p+1} = -\alpha - \beta i \qquad (57)$$

$$\alpha = \frac{\beta}{100} \qquad (58)$$

with imaginary parts β covering the frequency range of interest. The frequencies are scaled in gigahertz. The weighted linear cost function (4) is solved using the orthonormal rational basis functions (37)–(39), and an estimate for the residues c_p and $\tilde{c}_p$ is obtained. Using the residues $\tilde{c}_p$ and the poles $-a_p$, the minimal state-space realization (A, B, C, D) of the denominator $D(s)$(43) is calculated. From this state-space model, the poles of the transfer function are calculated by solving the eigenvalues of A-BC. These poles are chosen as new starting poles, and the method iterates until the poles are converged to their optimal location. Once the poles are known, the residues of the transfer function c_p can be estimated by solving (55) or (56).

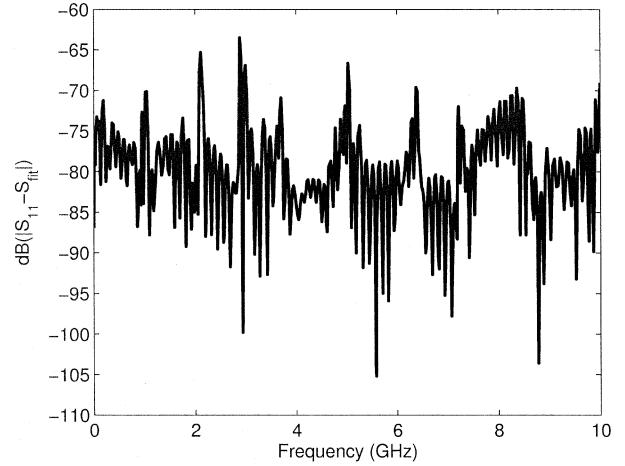In this example, the number of poles was set equal to 86, and the model is approximated by an improper transfer function in a least squares sense, using four SK-iterations. The final accuracy of the model is shown in Fig. 3, and the error

$$\text{Error} = \max(dB(|S_{11} - S_{\text{fit}}|)) \qquad (59)$$

corresponds to -63 dB, which is quite close to the numerical noise level of the simulator. Table I compares the condition numbers of the pole identification for VF and OVF in each iteration, when the initial poles are chosen optimally.

In [1], it was shown that the system equations become severely ill-conditioned if the real part of the starting poles is chosen nonnegligible. Fig. 4 shows a comparison of these condition numbers, and Fig. 5 shows a comparison of the RMS error, if the starting poles are chosen real, and equally spread over the (scaled) frequency range of interest. The transfer function is chosen to be a proper rational function. Note that the pole identification of OVF is significantly better conditioned, and leads to more accurate fitting models, compared to classical VF. To obtain an RMS error below the order of 10^{-3}, VF needed 13 iterations, while OVF could calculate such a fit using seven iterations. This leads to a reduction of approximately 46% in computation time.

When the starting poles are chosen complex conjugate, with a nonnegligible real part, similar conclusions can be made. As an example, Table II compares the condition numbers of the pole-identification when the real part of the starting poles is varied from to -0.2 to -1. The imaginary parts are equally spread over the (scaled) frequency range of interest. Clearly, the condition number rises for both methods as the distance to the imaginary axis increases. However, VF becomes severely ill-conditioned
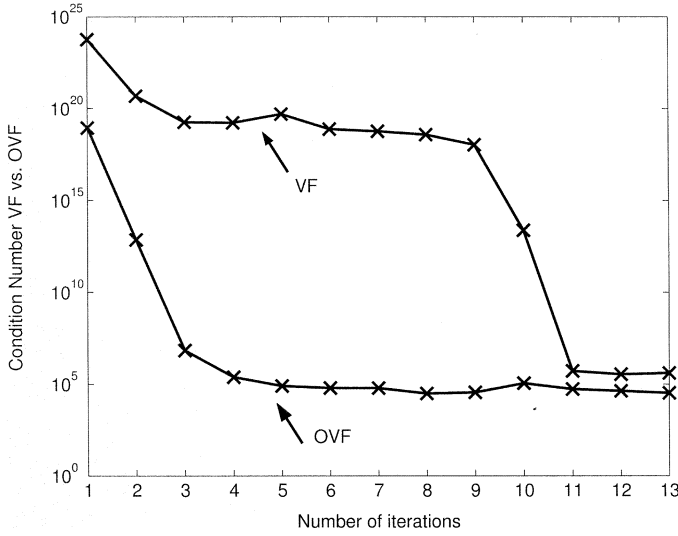
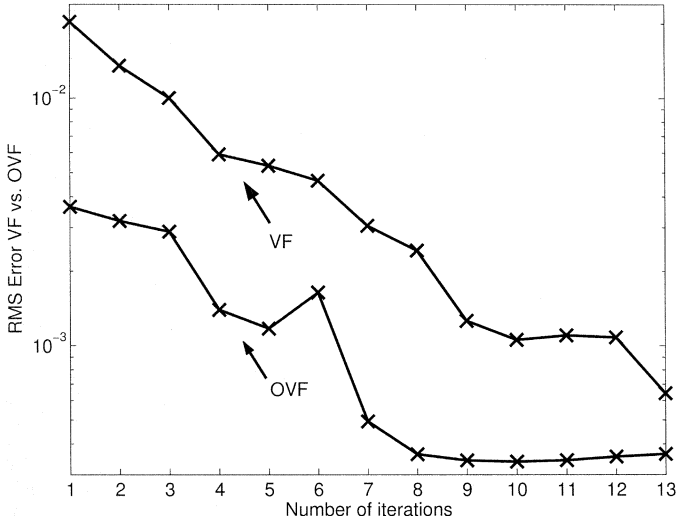Fig. 4. Condition number VF versus OVF per iteration—real starting poles.

Fig. 5. RMS Error VF versus OVF per iteration—real starting poles.

(e.g., when the real part of the poles is set to -1), while OVF still remains quite accurate.

Some further improvements in numerical conditioning can be obtained (for VF, as well as OVF) if the columns of the system equations are normalized to unit length.

VI. CONCLUSION

This paper introduces the orthonormal vector fitting technique, which builds accurate compact macromodels based on

TABLE II
CONDITIONING VERSUS. POLE LOCATION—COMPLEX CONJUGATE
STARTING POLES WITH VARYING REAL PARTS

$\Re e(-a_p)$	Cond.Nr. VF	Cond.Nr. OVF
-1	1.7233×10^{18}	1.6000×10^{8}
-0.8	8.7904×10^{16}	1.7145×10^{7}
-0.6	1.0795×10^{15}	1.8878×10^{6}
-0.4	5.0592×10^{12}	2.1849×10^{5}
-0.2	1.6968×10^{10}	3.2315×10^{4}

frequency-domain data samples. The method enhanced the numerical stability of vector fitting, by using orthonormal rational functions instead of partial fractions. This approach leads to significantly better conditioned equations when the initial choice of starting poles is not optimal. It limits the number of required iterations and the overall macromodeling time. The model is represented as state-space realization, which can easily be converted to a SPICE or EMTP circuit.

APPENDIX A
SANATHANAN-KOERNER ITERATION

The least-squares SK-cost function is defined as

$$\arg \min_{N_n^{(t)}, D_d^{(t)}} \left(\sum_{k=0}^{K} \left| \frac{1}{D^{(t-1)}(s_k)} \right|^2 \right.$$
$$\left. \times \left| D^{(t)}(s_k) H(s_k) - N^{(t)}(s_k) \right|^2 \right). \quad (60)$$

If the basis functions are chosen as partial fractions, based on a prescribed set of poles $-a_1, \ldots, -a_P$, then it follows that

$$N^{(t)}(s) = \sum_{p=1}^{P} \frac{c_p^{(t)}}{s + a_p} = \frac{\prod_{p=1}^{P-1} \left(s + z_{p,n}^{(t)} \right)}{\prod_{p=1}^{P} (s + a_p)} \quad (61)$$

$$D^{(t)}(s) = \sum_{p=1}^{P} \frac{\tilde{c}_p^{(t)}}{s + a_p} + \tilde{c}_0^{(t)} = \frac{\prod_{p=1}^{P} \left(s + z_{p,d}^{(t)} \right)}{\prod_{p=1}^{P} (s + a_p)}. \quad (62)$$

The denominator has an additional basis function, which equals the constant value 1. In the first iteration step $(t = 0)$, a Kalman linearization is applied to obtain a first guess of the denominator $(D^{(-1)}(s) = 1)$, as shown in (63) and (64), found at the bottom of the page. This reduces to solving the following set of least-squares equations, for all complex frequencies s

$$\left(\sum_{p=1}^{P} \frac{\tilde{c}_p^{(0)}}{s + a_p} + \tilde{c}_0^{(0)} \right) H(s) - \sum_{p=1}^{P} \frac{c_p^{(0)}}{s + a_p} = 0. \quad (65)$$

$$\arg \min_{N_n^{(t)}, D_d^{(t)}} \left(\sum_{k=0}^{K} \left| \frac{1}{D^{(t-1)}(s_k)} \right|^2 \left| D^{(t)}(s_k) H(s_k) - N^{(t)}(s_k) \right|^2 \right) \quad (63)$$

$$= \arg \min_{\tilde{c}_p^{(0)}, c_p^{(0)}} \left(\sum_{k=0}^{K} \left| \left(\sum_{p=1}^{P} \frac{\tilde{c}_p^{(0)}}{s_k + a_p} + \tilde{c}_0^{(0)} \right) H(s_k) - \sum_{p=1}^{P} \frac{c_p^{(0)}}{s_k + a_p} \right|^2 \right) \quad (64)$$

One coefficient of the rational function, e.g., $\tilde{c}_0^{(0)}$, can be fixed to unity, since numerator and denominator can be divided by the same complex value without loss of generality. So, (65) is equivalent to

$$\sum_{p=1}^{P} \frac{c_p^{(0)}}{s + a_p} - \sum_{p=1}^{P} \frac{\tilde{c}_p^{(0)}}{s + a_p} H(s) = H(s). \qquad (66)$$

Once the parameters $c_p^{(0)}$ and $\tilde{c}_p^{(0)}$ are estimated, $N^{(0)}(s)$ and $D^{(0)}(s)$ are known (61) and (62). It's straightforward to calculate $z_{p,n}^{(0)}$ and $z_{p,d}^{(0)}$ in a robust way, by solving the eigenvalue problem (24). In practice, only $z_{p,d}^{(0)}$ is needed.

Now, the Sanathanan–Koerner linearization can be applied for iteration step $t = 1, \ldots, T$, as shown in (67)–(70), found at the bottom of the page. Note that the poles of $N^{(t)}(s)$ and $D^{(t)}(s)$ remain unchanged, and cancel out in each iteration (68). Again, this reduces to solving the following set of least-squares equations, for all complex frequencies s

$$\sum_{p=1}^{P} \frac{d_p^{(t)}}{s + z_{p,d}^{(t-1)}} - \sum_{p=1}^{P} \frac{\tilde{d}_p^{(t)}}{s + z_{p,d}^{(t-1)}} H(s) = H(s). \qquad (71)$$

In successive iterations ($t>0$), the coefficients $\tilde{d}_p^{(t)}$ of $D^{(t)}/D^{(t-1)}$ are used to calculate the poles. This does not pose a problem, as the zeros of $D^{(t)}$ and $D^{(t)}/D^{(t-1)}$ are the same.

APPENDIX B
REAL-VALUED STATE SPACE

This appendix describes how the real-valued state-space realization of

$$\frac{(s - a_p^*)(s - a_{p+1}^*)}{(s + a_p)(s + a_{p+1})} = 1 + \frac{4\Re e(-a_p)s}{(s + a_p)(s + a_p^*)} \qquad (72)$$

can be obtained.

Define the state matrix A and input vector B as

$$A = \begin{pmatrix} A_{11} & A_{12} \\ A_{21} & A_{22} \end{pmatrix} \qquad B = \begin{pmatrix} B_1 \\ B_2 \end{pmatrix} \qquad (73)$$

where A_{ij} and B_i are the scalar elements of the matrix and the vector, respectively. Capitals are used to avoid notational confusion between the poles and the entries of the state matrix.

A first constraint on the entries, is that the poles of (72), $\{-a_p, -a_p^*\}$, must equal the eigenvalues of A. More specifically, the transfer function from the input $U_1(s)$ and $U_2(s)$ to the states $X_1(s)$ and $X_2(s)$, respectively, must satisfy

$$\frac{X_1(s)}{U_1(s)} = \frac{s - |a_p|}{(s + a_p)(s + a_p^*)} \qquad (74)$$

$$\frac{X_2(s)}{U_2(s)} = \frac{s + |a_p|}{(s + a_p)(s + a_p^*)}. \qquad (75)$$

The input-to-state transfer function is given by

$$\frac{X(s)}{U(s)} = (sI - A)^{-1}B \qquad (76)$$

$$= \frac{\begin{pmatrix} s - A_{22} & A_{12} \\ A_{21} & s - A_{11} \end{pmatrix}}{(s - A_{11})(s - A_{22}) - A_{12}A_{21}}B. \qquad (77)$$

So

$$\frac{X_1(s)}{U_1(s)} = \frac{(s - A_{22})B_1 + A_{12}B_2}{(s - A_{11})(s - A_{22}) - A_{12}A_{21}} \qquad (78)$$

and

$$\frac{X_2(s)}{U_2(s)} = \frac{A_{21}B_1 + (s - A_{11})B_2}{(s - A_{11})(s - A_{22}) - A_{12}A_{21}}. \qquad (79)$$

By equating the numerators of (74) to (78), (75) to (79), and applying some basic linear algebra, the following constraints are easily obtained

$$B_1 = 1 \qquad (80)$$
$$B_2 = 1 \qquad (81)$$
$$-A_{22} + A_{12} = -|a_p| \qquad (82)$$
$$A_{21} - A_{11} = |a_p| \qquad (83)$$

which determine the input vector B completely. Unfortunately, the elements of the state matrix A are still ambiguous.

$$\arg \min_{N_n^{(t)}, D_d^{(t)}} \left(\sum_{k=0}^{K} \left| \frac{1}{D^{(t-1)}(s_k)} \right|^2 \left| D^{(t)}(s_k)H(s_k) - N^{(t)}(s_k) \right|^2 \right) \qquad (67)$$

$$= \arg \min_{z_{p,n}^{(t)}, z_{p,d}^{(t)}} \left(\sum_{k=0}^{K} \left| \frac{\prod_{p=1}^{P}(s_k + a_p)}{\prod_{p=1}^{P}\left(s_k + z_{p,d}^{(t-1)}\right)} \right|^2 \left| \left(\frac{\prod_{p=1}^{P}\left(s_k + z_{p,d}^{(t)}\right)}{\prod_{p=1}^{P}(s_k + a_p)} \right) H(s_k) - \frac{\prod_{p=1}^{P-1}\left(s_k + z_{p,n}^{(t)}\right)}{\prod_{p=1}^{P}(s_k + a_p)} \right|^2 \right) \qquad (68)$$

$$= \arg \min_{z_{p,n}^{(t)}, z_{p,d}^{(t)}} \left(\sum_{k=0}^{K} \left| \left(\frac{\prod_{p=1}^{P}\left(s_k + z_{p,d}^{(t)}\right)}{\prod_{p=1}^{P}\left(s_k + z_{p,d}^{(t-1)}\right)} \right) H(s_k) - \frac{\prod_{p=1}^{P-1}\left(s_k + z_{p,n}^{(t)}\right)}{\prod_{p=1}^{P}\left(s_k + z_{p,d}^{(t-1)}\right)} \right|^2 \right) \qquad (69)$$

$$= \arg \min_{\tilde{d}_p^{(t)}, d_p^{(t)}} \left(\sum_{k=0}^{K} \left| \left(\sum_{p=1}^{P} \frac{\tilde{d}_p^{(t)}}{s_k + z_{p,d}^{(t-1)}} + \tilde{d}_0^{(t)} \right) H(s_k) - \sum_{p=1}^{P} \frac{d_p^{(t)}}{s_k + z_{p,d}^{(t-1)}} \right|^2 \right) \qquad (70)$$

By equating the denominators, it follows that

$$s^2 - (A_{11} + A_{22}) + (A_{11}A_{22} + A_{12}A_{21}) \qquad (84)$$
$$= s^2 + \left(a_p + a_p^*\right) + a_p a_p^* \qquad (85)$$

so

$$A_{11} + A_{22} = -2\Re e(a_p) \qquad (86)$$
$$A_{11}A_{22} - A_{12}A_{21} = |a_p|^2. \qquad (87)$$

Combining (87) with (82) and (83)

$$A_{11} - A_{12} = |a_p|. \qquad (88)$$

Using (82) and (88)

$$A_{11} - A_{22} = 0 \qquad (89)$$
$$A_{11} = A_{22}. \qquad (90)$$

Obviously from (86) and (90), it results that

$$A_{11} = \Re e(-a_p) \qquad (91)$$
$$A_{22} = \Re e(-a_p). \qquad (92)$$

Combining this with (82) and (83), it follows that

$$A_{12} = \Re e(-a_p) - |a_p| \qquad (93)$$
$$A_{21} = \Re e(-a_p) + |a_p| \qquad (94)$$

which determines A uniquely.

Verifying that the eigenvalues of A are actually equal to $-a_p$ and $-a_p^*$ is trivial.

Now, C and D can easily be formed to obtain (72)

$$C = \left(\, 2\Re e(-a_p) \quad 2\Re e(-a_p) \,\right), \quad D = 1 \qquad (95)$$

REFERENCES

[1] B. Gustavsen and A. Semlyen, "Rational approximation of frequency domain responses by vector fitting," *IEEE Trans. Power Delivery*, vol. 14, no. 3, pp. 1052–1061, Jul. 1999.

[2] C. K. Sanathanan and J. Koerner, "Transfer function synthesis as a ratio of two complex polynomials," *IEEE Trans. Autom. Control*, vol. AC-8, no. 1, pp. 56–58, Jan. 1963.

[3] W. Hendrickx and T. Dhaene, "A discussion of rational approximation of frequency domain reponses by vector fitting," *IEEE Trans. Power Syst.*, vol. 21, no. 1, pp. 441–443, Feb. 2006.

[4] D. Deschrijver and T. Dhaene, "Rational modeling of spectral data using orthonormal vector fitting," in *Proc. 9th IEEE Workshop Signal Propagation on Interconnects*, 2005, pp. 111–114.

[5] R. Pintelon and J. Schoukens, *System Identification: A Frequency Domain Approach*. Piscataway, NJ: IEEE Press, 2000.

[6] G. H. Golub and C. F. Van Loan, *Matrix computations*, 3rd ed. London, U.K.: The Johns Hopkins University Press, 1996.

[7] R. Pintelon, P. Guillaume, Y. Rolain, J. Schoukens, and H. V. Hamme, "Parametric identification of transfer functions in the frequency domain—A survey," *IEEE Trans. Autom. Control*, vol. 39, no. 11, pp. 2245–2260, Nov. 1994.

[8] B. Wahlberg and P. Makila, "On approximation of stable linear dynamical systems using laguerre and Kautz functions," *Automatica*, vol. 32, pp. 693–708, 1996.

[9] K. Levenberg, "A method for the solution of certain problems in least squares," *Quart. J. Appl. Math.*, vol. 2, pp. 164–168, 1944.

[10] D. Marquardt, "An algorithm for least-squares estimation of nonlinear parameters," *SIAM J. Appl. Math.*, vol. 11, pp. 431–441, 1963.

[11] H. Akcay and B. Ninness, "Orthonormal basis functions for modelling continuous-time systems," *Signal Process.*, vol. 77, no. 1, pp. 261–274, 1999.

[12] R. E. Kalman, "Design of a self optimizing control system," *Trans. ASME*, vol. 80, pp. 468–478, 1958.

[13] E. C. Levi, "Complex curve fitting," *IEEE Trans. Autom. Control*, vol. AC-4, no. 1, pp. 37–43, Jan. 1959.

[14] A. H. Whitfield, "Asymptotic behavior of transfer function synthesis methods," *Int. J. Control*, vol. 45, pp. 1083–1092, 1987.

[15] J. Adcock and R. Potter, "A frequency domain curve fitting algorithm with improved accuracy," in *Proc. 3rd Int. Modal Anal. Conf.*, 1985, vol. 1, pp. 541–547.

[16] M. Richardson and D. L. Formenti, "Parameter estimation from frequency response measurements using rational fraction polynomials," in *Proc. 1st Int. Modal Anal. Conf.*, 1982, pp. 167–182.

[17] Y. Rolain, R. Pintelon, K. Q. Xu, and H. Vold, "Best conditioned parametric identification of transfer function models in the frequency domain," *IEEE Trans. Autom. Control*, vol. 40, no. 11, pp. 1954–1960, Nov. 1995.

[18] B. Gustavsen, "Improving the pole relocating properties of vector fitting," *IEEE Trans. Power Delivery*, vol. 21, no. 3, pp. 1587–1592, Jul. 2006.

[19] W. Hendrickx, D. Deschrijver, and T. Dhaene, "Some remarks on the vector fitting iteration," in *Post-Conf. Proc. EMCI 2004, Mathematics in Industry*, 2006, vol. 8, pp. 134–138.

[20] B. Ninness, S. Gibson, and S. R. Weller, "Practical aspects of using orthonormal system parameterisations in estimation problems," in *Proc. 12th IFAC Symp. Syst. Ident.*, 2000.

[21] D. Deschrijver and T. Dhaene, "Broadband macromodelling of passive components using orthonormal vector fitting," *Electron. Lett.*, vol. 41, no. 21, pp. 1160–1161, 2005.

[22] L. Knockaert, "On orthonormal Muntz–Laguerre filters," *IEEE Trans. Signal Process.*, vol. 49, no. 4, pp. 790–793, Apr. 2001.

[23] T. Oliveira e Silva, Rational Orthonormal Functions on the Unit Circle and on the Imaginary Axis, with Applications in System Identification University of Aveiro, Aveiro, Portugal, Tech. Rep., Oct. 2005.

[24] S. Takenaka, "On the orthogonal functions and a new formula of interpolation," *Jpn. J. Math.*, pp. 129–145, 1925.

[25] F. Malmquist, "Sur la détermination d'une classe de fonctions analytiques par leurs valeurs dans un ensemble donné de points," in *Compte Rendus Sixieme Congr. Math. Scand.*, 1926, pp. 253–259.

[26] P. R. Clement, "Laguerre functions in signal analysis and parameter identification," *J. Franklin Inst.*, vol. 313, pp. 85–95, 1982.

[27] W. H. Kautz, "Transient synthesis in the time-domain," *IRE Trans. Circuit Theory*, vol. 1, pp. 29–39, 1954.

[28] P. S. C. Heuberger, P. M. J. Van Den Hof, and B. Wahlberg, *Modelling and Identification With Rational Orthogonal Basis Functions*. London: Springer-Verlag, 2005.

[29] J. C. Gomez, "Analysis of dynamic system identification using rational orthonormal bases," Ph.D. dissertation, Univ. Newcastle, Newcastle, NSW, Australia, 1998.

Dirk Deschrijver was born in Tielt, Belgium, on September 26, 1981. He received the M.S. degree in computer science from the University of Antwerp, Antwerp, Belgium, in 2003.

Since then, he has been working at the Computer Modeling and Simulation (COMS) Group, University of Antwerp, supported by a research project of the Fund for Scientific Research, Flanders (FWO-Vlaanderen). His research interests include rational least-squares approximation, system identification using orthonormal rational functions, and macromodeling. From May to October 2005, he was a Marie Curie Fellow at the Eindhoven University of Technology, Eindhoven, The Netherlands.

Bart Haegeman was born in Tienen, Belgium, on October 27, 1975. He received the M.S. degree in electrotechnical engineering, the M.S. degree in physics, and the Ph.D. degree in physics, all from the Katholieke Universiteit Leuven (KULeuven), Leuven, Belgium, in 1998, 2000, and 2004, respectively.

From 2000 to 2004, he was a Research Assistant for the Fund for Scientific Research, Flanders, in the Institute for Theoretical Physics, KULeuven. He has been working on several mathematical modeling problems, ranging from laser dynamics, quantum computers, car transmission systems, and high-speed electronic components, both in academic and industrial settings. Currently, he is working on a project in microbial ecology as a Postdoctoral Fellow at INRIA Sophia, Antipolis, France.

Tom Dhaene was born in Deinze, Belgium, on June 25, 1966. He received the Ph.D. degree in electrotechnical engineering from the University of Ghent, Ghent, Belgium, in 1993.

From 1989 to 1993, he was Research Assistant at the University of Ghent, in the Department of Information Technology, where his research focused on different aspects of full-wave electromagnetic circuit modeling, transient simulation, and time-domain characterization of high-frequency and high-speed interconnections. In 1993, he joined the EDA company Alphabit (now part of Agilent). He was one of the key developers of the planar EM simulator ADS Momentum, and he is the principal developer of the multivariate EM-based adaptive metamodeling tool ADS Model Composer. Since September 2000, he has been a Professor in the Computer Modeling and Simulation (COMS) Group, University of Antwerp, Antwerp, Belgium, in the Department of Mathematics and Computer Science. His modeling and simulation EDA software is successfully used by academic, government, and business organizations worldwide, for study and design of high-speed electronics and broadband communication systems. As author or co-author, he has contributed to more than 100 peer-reviewed papers and abstracts in international conference proceedings, journals, and books. He is the holder of two U.S. patents.